CrystEngComm

Accepted Manuscript

ROYAL SOCIETY OF CHEMISTRY

www.rsc.org/crystengcomm

CrystEngComm RSCPublishing

ARTICLE

Morphology control and fabrication of multi-shelled NiO spheres by tuning pH value via hydrothermal process

Cite this: DOI: 10.1039/x0xx00000x

Received 00th August 2014,
Accepted 00th October 2014

DOI: 10.1039/x0xx00000x

www.rsc.org/

Lihua Chu,[a] Meicheng Li,[*a,b] Zipei Wan,[a] Lei Ding,[c] Dandan Song,[a] Shangyi Dou,[a] Jiewei Chen,[a] Yu Wang[a]

Controlling the morphology of nickel oxide (NiO) nanostructures is crucial to obtain excellent physical and chemical performance. Hence, the morphology of NiO was tuned by adjusting the pH value of the precursor solutions with $NH_3 \cdot H_2O$, via hydrothermal process and subsequent calcination. Different morphologies, including nanoparticles, porous structure and multi-shelled microsphere, were obtained with the pH values varied from 8.30 to 10.90. The morphology evolution of as synthesized NiO with the pH value indicates the important role of OH^- in controlling the product morphology. Moreover, the formation mechanism of different NiO nanostructures at different pH values was discussed. Furthermore, the surface area and magnetic properties of the NiO with different morphologies were also investigated, and indeed, these properties are very sensitive to the morphology. This work provides a facile way to control the morphology of NiO nanostructures, which also implies the potential application in modern science and technology with the modified magnetic properties.

Introduction

Nickel oxide (NiO), as one of limited p-type wide-band gap (3.6–4.0 eV) semiconductor metal oxides, is a very promising material and has recently received considerable attention due to its significant importance in both fundamental research and applications, including antiferromagnetic materials,[1] gas sensors,[2,3] catalysis,[4] and battery electrodes.[5] In most potential applications, the quality and structure of the nanomaterials undoubtedly play the crucial role in determining their functions. With rising interest in engineering the morphology of NiO nanomaterials during the past decade, it is found that the performance of NiO nanomaterials is also deeply affected by its morphology characteristics.[6-8] For instance, the magnetic properties of the NiO nanostructure, containing spin configuration, superparamagnetism and magnetic hysteresis, were observed to depend on its morphology characteristics including the size and the architecture.[7-10] Hence, many efforts have focused on exploiting fabrication procedures of NiO nanostructures with different morphologies, which can be controlled by designed functionalities. NiO nanostructures could be fabricated by hydrothermal routes,[11] reflux method,[12] thermal decomposition[13], chemical precipitation[14] and electro spinning method.[15] Among these methods, the hydrothermal synthesis, without special high temperature conditions or tedious procedures, has become one of the mostly used methods to obtain inorganic nanomaterials, such as metal nanomaterials and their oxide nanomaterials.[11,16,17]

As one of the key factors in hydrothermal process, the pH value of the precursor solution plays an essential role in determining the morphology of nanostructures. For instance, Sun and Zhu et al. have demonstrated that pH value plays an important role for the morphology of $Ni(OH)_2$ in the hydrothermal system.[2, 18] It was found that high pH value, i.e. the pH value of 11.0, is in favor of the formation of free-standing $Ni(OH)_2$ nanoplatelets. A suitable pH value was instrumental in fabrication of the lotus-root-like NiO nanosheets and three-dimensional flower-like NiO microspheres.[9] Assisted by aqueous ammonia ($NH_3 \cdot H_2O$), single-crystalline β-$Ni(OH)_2$ nanosheets with hexagonal structure were synthesized.[19] These obtained $Ni(OH)_2$ nanostructures with different morphologies can be transferred into NiO without the structural deformation. In spite of these pioneering reports of the effect of pH value on morphology, it is still a challenge to precisely control the morphology characteristics including the size and the architecture of NiO nanostructures by adjusting the pH values. In addition, comparing with the widely investigated factors containing reaction rate, temperature, chelating reagent, precursor solution concentration,[11] the effect mechanism of the pH value on the morphology is not fully understood.

Herein, we tuned the morphology of the nanosized NiO materials by tailoring the pH value of the precursor solution via hydrothermal routes. Furthermore, the influence of pH value on the morphology evolution of NiO nanostructures has been investigated and the possible formation mechanism was discussed. Moreover, the influence of the morphology on the

magnetic properties of as synthesized NiO products was investigated, and it was found that the magnetic properties of NiO are very sensitive to its morphology characteristics.

Experimental

Preparation

The NiO products were prepared by precipitation and a hydrothermal process. All reagents used in the experiments were in analytical grade and used without further purification. Distilled water was used for all synthesis and treatment processes. The preparation of $Ni(OH)_2$ was performed as follows. Typically, 1 g of $Ni(NO)_3 \cdot 6H_2O$ and 1 g of D-Glucose were dissolved in 30 mL of distilled water, adjusting the pH value to 8.30, 8.60, 9.30, 10.30, 10.50 and 10.90 with $NH_3 \cdot H_2O$, using a pH meter and magnetic stirrer to form a homogeneous solution at room temperature. The solution was then transferred into a Teflon-lined stainless steel autoclave (50 mL), sealed, and heated at 150 ºC for 15 h. The product was collected by centrifugation, washed with deionized water and ethanol several times to remove impurity, and then dried at 60 ºC in vacuum. Finally, the NiO nanostructures were obtained by heating the hydroxide precursor at 500 ºC for 6 h in air.

Characterization

The morphology of as synthesized NiO nanostructures was observed by FEI Quanta 200F microscope field emission scanning electron microscope (FESEM) and Tecnai G2 F20 Field emission transmission electron microscopy (TEM) with accelerating voltage of 200 kV. The crystalline phase was identified by a Bruker D8 Focus X-ray powder diffractometer with using Cu K_α(λ =1.5406Å) radiation over a range of 2θ from 20º to 90º. The thermogravimetric/differential thermal analysis (TG/DTA) measurement was performed using STA6000 thermogravimertic analyzer in air at a scan rate of 10 °C/min from room temperature to 600 °C. Brunauer-Emmett-Teller (BET) surface areas of the samples were analyzed by nitrogen adsorption–desorption measurement on a Quantachrome Autosorb-IQ-MP sorption analyzer with prior degassing under vacuum at 77K. Pore size distribution was derived from desorption branch by a BJH method. The temperature dependence of the magnetization was measured between 10 K and 400 K under magnetic field of 500 Oe, using the superconducting quantum interference device (SQUID) magnetometer (Quantum Design MPMS-XL). The measurement was conducted under both zero field cooling (ZFC) and field cooling (FC) conditions. A set of isothermal magnetization M(H) at selected temperatures was measured between -70 kOe and 70 kOe, in the same apparatus.

Results and discussion

To study the effect pH value on the morphology, the morphologies and detailed crystal structures of as prepared NiO nanostructures at different pH values were analyzed by scanning electron microscopy (SEM), transmission electron microscopy (TEM) and powder X-ray diffraction (XRD). Fig. 1 depicts the FESEM images of the NiO nanostructures synthesized at different pH values. As shown in Fig. 1(a), NiO nanoparticles were obtained at the pH value of 8.30. Fig. 1(b) and (c) shows the morphology of NiO prepared at the pH value of 8.60, which presents that the NiO nanoparticles start to aggregate together to form porous clusters. With the increasing of the pH value, the aggregation become more and more significant, and the number of micro holes is decreased, as can be seen from Fig. 1(d) and (e). When the pH value reached to 10.50, the hollow microspheres were obtained (Fig. 1f). When a further increase of the pH value to 10.90, the microsphere, with the diameter varied from 2.0 μm to 3.5 μm, exhibits smooth and compact surface. The microsphere has multi-shelled structure as shown in Fig. 1(f) inset. The intermediate product, $Ni(OH)_2$ microspheres, was also characterized by FESEM, as shown in Fig. 1(g). It is clear that the morphology can be well-sustained during the transformation process from $Ni(OH)_2$ to NiO, without being damaged to dispersive nanoparticles or other morphologies. The morphology evolution of NiO with the pH value of the precursor solution indicates the significant influence of pH value on the morphology of the products.

The crystal structure and purity of as prepared NiO products via hydrothermal method at different pH values were examined by powder XRD, as shown in Fig. 2. Here, the NiO products prepared under the pH values of 9.30 and 10.90 were used as the examples. All the diffraction peaks observed can be perfectly indexed to the pure NiO products with face centered cubic phase (JCPDS No 47-1049, space group Fm3m). The diffraction peaks correspond to the (111), (200), (220), (311) and (222) planes, respectively. No other peaks arising from impurities can be found, indicating that pure NiO crystals have been successfully synthesized. It can also be concluded that the crystal phase was not affected by the pH value.

To obtain insight into the morphology characteristics of the porous and NiO spheres, TEM technique was used to visualize the detailed structure of as prepared multi-shelled NiO spheres. The TEM images are shown in Fig. 3. The porous NiO is composed of NiO nanoparticles, as shown in Fig. 3(a) and (b). The micrograph of Fig. 3(c)-(d) shows that the microsphere has a hollow structure with multi-shells, in accordance with the SEM pattern in Fig. 1(f). The microsphere has 3-5 shells with the shell thickness approximate 50 nm. The HRTEM image of a typical microsphere and its corresponding Fast Fourier Transform (FFT) pattern are shown in Fig. 3(d). Well-resolved lattice fringes in the HRTEM image correspond to the interplanar spacing of 2.4 Å, 2.0 Å, 1.5 Å, consistent with the (111), (200), (220) planes of NiO crystal.

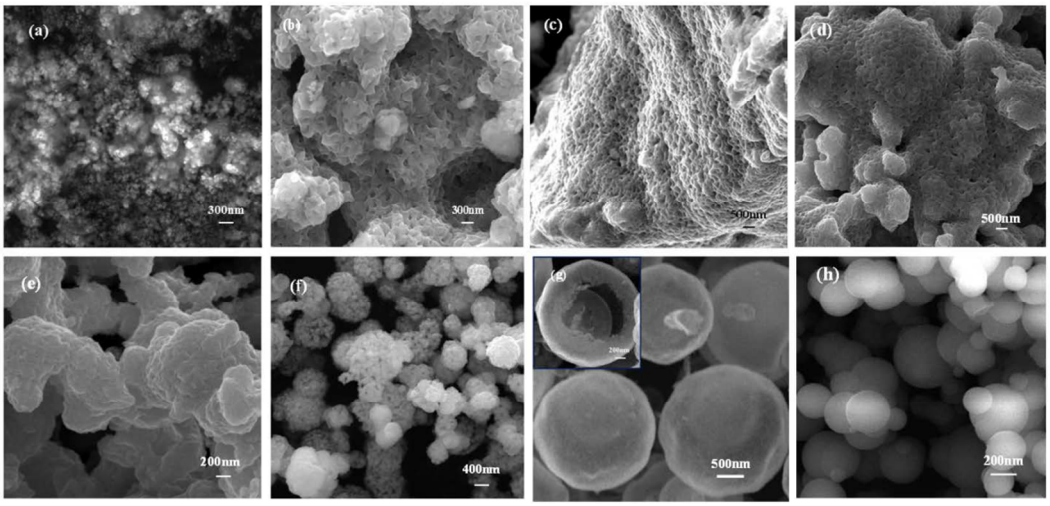

Fig. 1 (a)-(g) SEM images of NiO prepared by hydrothermal synthesis at different pH values (a) pH=8.30, (b) and (c) pH=8.60, (d) pH=9.30, (e) pH=10.30, (f) pH=10.50, (g) pH=10.90; (h) SEM image of the precursor $Ni(OH)_2$ prepared at pH=10.90

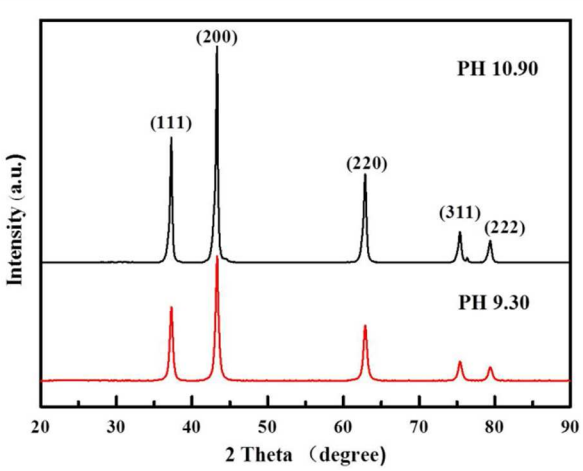

Fig. 2 Room temperature XRD patterns of as synthesized NiO products via hydrothermal synthesis at the pH value of 9.30 and 10.90.

The formation process of NiO from the solution with $Ni(NO)_3 \cdot 6H_2O$ and D-Glucose as the reactants is explained as follows. Initially, Ni^{2+} ions create relatively stable complexes $[Ni(NH_3)_x]^{2+}$ with $NH_3 \cdot H_2O$, meanwhile, the rate of the crystal growth will be low due to the decrease of the concentration of free Ni^{2+}. Then the complexes decompose and release NH_3 to provide OH^- ions for the formation of $Ni(OH)_2$ in hydrothermal condition.[9, 20] After the calcination at 500℃ for 6h in air, $Ni(OH)_2$ was converted to NiO. The reactions can be formulated as demonstrated below:

$$Ni^{2+} + xNH_3 \cdot H_2O \rightarrow [Ni(NH_3)_x]^{2+} + 6H_2O \quad (1)$$

$$[Ni(NH_3)_x]^{2+} \rightarrow Ni^{2+} + x(NH_3) \quad (2)$$

$$NH_3 \cdot H_2O \rightarrow NH_4^+ + OH^- \quad (3)$$

$$Ni^{2+} + 2OH^- \rightarrow Ni(OH)_2 \quad (4)$$

$$2Ni(OH)_2 + O_2 \rightarrow 2NiO + 2H_2O \quad (5)$$

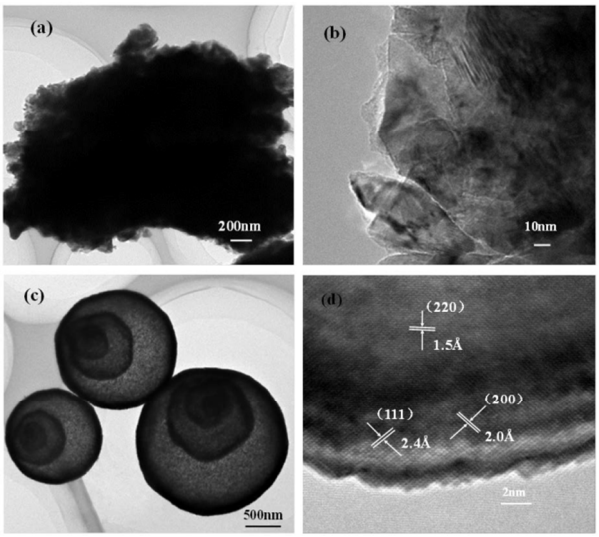

Fig. 3 TEM images of as prepared NiO at different pH values (a-b) the porous NiO prepared by pH=8.60 (c) the multi-shelled NiO spheres produced by pH=10.90 and (d) HRTEM of multi-shelled NiO spheres.

The thermal decomposition behavior of as synthesized $Ni(OH)_2$ microsphere precursor was evaluated to study the conversion process, through TG/DTA measurement, and the TG/DTA curves are shown in Fig. 4. The initial weight loss of 11.79% was observed in the temperature range of 50-180 °C, which was mainly caused by the loss of physically absorbed water within the $Ni(OH)_2$ microspheres. There are obviously two steps of weight loss of 74.14% occurring between 180 and 430 °C (endothermic peak at 405 °C in the derivative weight curve), which are attributed to the thermal decomposition of $Ni(OH)_2$ to NiO and the combustion of carbon in the microspheres. No weight loss could be observed above 430 °C. Thus, it is concluded that the $Ni(OH)_2$ precursor can decompose to form NiO at above 405 °C. The calcining temperature was

500 °C in our experiment, and thus pure NiO phase was obtained.

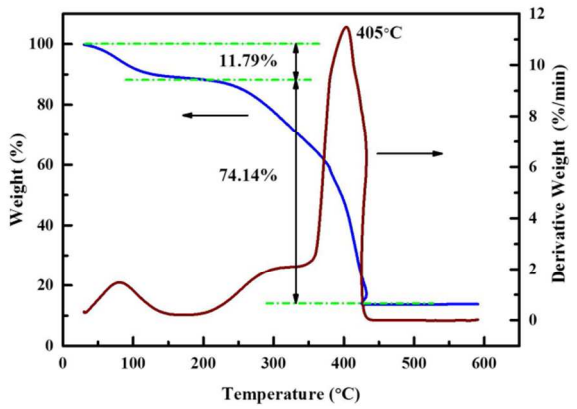

Fig. 4 The TG/DTA curves of the $Ni(OH)_2$ spheres with multi-shelled structure prepared at pH=10.90.

During the hydrothermal process, the carbon spheres were formed simultaneously from glucose in the solution involving the dehydration of the carbohydrate.[21] The surface of the carbon spheres is hydrophilic and attached by a number of OH^- groups, and hence, the carbon spheres are able to act as the templates for ion attaching in the following reaction processes. When the pH value of the precursor solution is low, such as 8.30, the solution appears weakly alkaline, and the $NH_3 \cdot H_2O$ provides a low concentration of OH^- ions for the formation of $Ni(OH)_2$, leading to the low growth rate of the crystal and the weak assembly or aggregating behaviour of the crystal nuclei. Meanwhile, the OH^- ions attached to the surface of carbon spheres are also limited, so the carbon spheres have minor effect on the morphology evolution of the product. Therefore, the $Ni(OH)_2$ nanoparticles of are preferentially formed at low pH value. In the cases of at middle pH values, i.e., 8.60, 9.30, 10.30, the solution generates more OH^- and a higher concentration of NH_3, Ni^{2+} and NH_3 have a stronger chelating ability than at pH the value of 8.30, resulting in a high growth rate of $Ni(OH)_2$ nuclei.[7] These nuclei therefore spontaneously attach together followed by the formation of aggregates to decrease the surface energy by reducing exposed areas, whereas this aggregation process is lack of self-orientation.[22] The effect of carbon spheres on the morphology is still faint weak at middle pH value, so the product is composed of porous and loose aggregates.

With further increasing the pH value of the precursor solution to 10.90, a much higher content of NH_3 react with Ni^{2+} to form a large quantity of relatively stable complex, $[Ni(NH_3)_y]^{2+}$, and the chelating ability is sufficiently strong during the hydrothermal treatment. Hence, the $[Ni(NH_3)_y]^{2+}$ complex is supersaturated in the solution, leading to the much higher growth rate of $Ni(OH)_2$ nuclei. Therefore, with the favor of the higher growth rate and the spontaneous energy-minimizing process by removing surface energy associated with unsatisfied bonds, the resulting $Ni(OH)_2$ nuclei gradually self-organized with further reacting. Subsequently, the $Ni(OH)_2$ nuclei formed and assembled to nanoparticles on the surface of carbon spheres based on the coalescence mechanism. Consequently, the inside-out Ostwald-ripening growth would dominate.[20] The schematic formation process is depicted in Fig. 5.

The second shell initially deposits on the first dense shell, and then, partial of the second shell around the interfacial region was dissolved due to the structural heterogeneity of the second shell, which results in higher surface energy compared with the primary homogenous shell[11, 23]. These double-shelled particles again act as templates for another run of $Ni(OH)_2$ nanoparticle deposition. With further ripening, outward migration of interfacial region results in continued expansion of the interior space within the original aggregates, and hence the interior void space of the spheres was further expanded. In addition, the external surface and outward migration of the interfacial region were also protected by the adsorbed NO_3^{2-} ions with oxidizing ability.[24, 25] Therefore, the multi-shelled $Ni(OH)_2$ hollow spheres were obtained. Additionally, the number of the shells and the inter-shell spacing are sensitive to many parameters such as reaction process, solvent, ionic concentration and so on.[26, 27] As the formation mechanism and the structure engineering of multi-shelled sphere are out of the research focus in this paper, they will be further discussed in our following work.

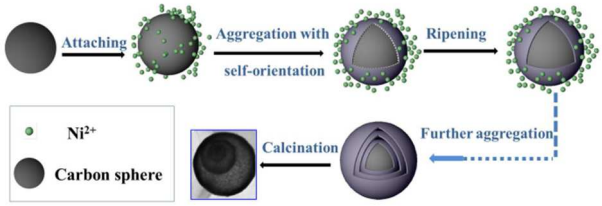

Fig. 5 Schematic illustration of the growth process of multi-shelled NiO microspheres obtained at pH 10.90 of the precursor solution

To further present specific textural properties of as prepared NiO nanostructures, the porosity of NiO products with different morphologies was also characterized by Brunauer-Emmett-Teller (BET) nitrogen adsorption-desorption analysis, as shown in Fig. 6. In terms of shape, the adsorption isotherm of all the three samples obtained at the pH values of 9.30, 10.30 and 10.90 are similar, which can be classified as type IV curves with a type Ⅲ hysteresis loops according to the IUPAC classification. The BET surface area was calculated to be 3.30 m^2/g for the NiO nanostructure prepared at the pH value of 9.30. Interestingly, with the increase in the pH value of precursor, the BET surface area of the samples is also increased to 6.78 m^2/g and 28.90 m^2/g for the sample prepared at the pH values of 10.30 and 10.90, respectively.

The magnetic properties of NiO nanostructures are highly dependent on the morphology characteristics,[9, 10] so the temperature dependence of the magnetization and isothermal magnetization of NiO with different morphology were also investigated. The temperature dependence of the magnetization curves M(T) for the

selective NiO products with different morphologies were measured at 500 Oe under zero field cooled (ZFC) and field cooled (FC) process as presented in Fig. 7(a)-(c). For Fig. 7(a) and (b), i.e. the NiO prepared at the pH value of 9.30 and 10.30, respectively, each of the ZFC magnetization curves shows a peak and a bifurcation with the corresponding FC magnetization curve below a certain temperature, as typically present in an assembly of ferromagnetic-like nanoparticles exhibiting superparamagnetism above a certain temperature.[26] The peak in the ZFC curve is usually associated with the blocking temperature (T_B) which increased with the pH value increasing (T_B≈275 K for pH=9.30, T_B≈316 K for pH=10.30). The peak of the multi-shelled NiO microspheres was not observed within the measurement range between 10 and 400K, as shown in Fig. 7(c), and it is probably located at the temperature higher than 400K from the variation tendency of the curve. The bifurcation between ZFC and FC magnetization curves deriving from surface effects is due to the presence of uncompensated surface spins. [28]

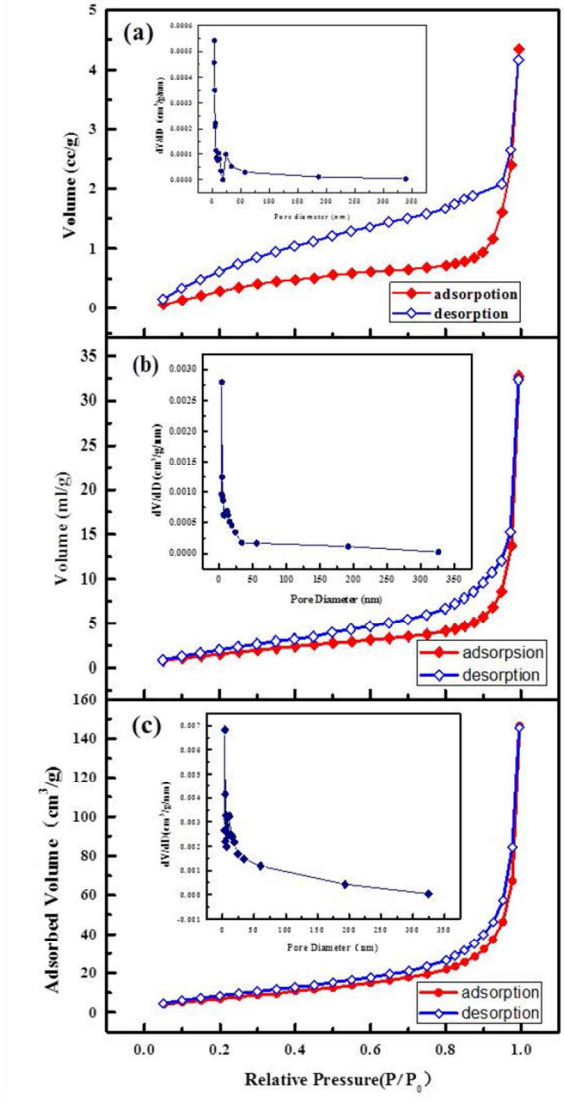

Fig. 6 Nitrogen adsorption-desorption isotherms of the NiO obtained by hydrothermal synthesis at different pH values. The inset shows BJH pore-size distributions: (a) pH=9.30(Total pore volume = 6.71×10^{-3}cc/g; Average pore Diameter = 8.11nm); (b) pH=10.30 (Total pore volume = 5.06×10^{-2} cc/g; Average pore size=0. 30 nm); (c) pH=10.90(Total pore volume = 2.26×10^{-1} cc/g; Average pore Diameter =0. 31 nm)

Isothermal Magnetization curves M(H) were also measured at various temperature (Fig. 7(d)-(f)). For the NiO prepared at the pH value of 9.30, the magnetization curves show typical ferromagnetic characteristics with a remnant magnetization (M_r) of 0.23 emu/g at 300K, which is quite different from the bulk sample.[29] The ferromagnetic property may be attributed to the size confinement effect of the NiO nanoparticles composed of small magnetic domains characterized by its own magnetic moment.[30] The magnetization curves of the NiO synthesized at the pH value of 10.30 display s-shapes without saturation indicating typical FIM behavior (Fig. 7(e)). The magnetization curves of the NiO prepared at the pH value of 10.90 in all of the test temperatures almost increases monotonously with increasing magnetic field, which is close to the typical antiferromagnetic characteristics, and exhibit bends at low magnetic field suggesting the presence of a tiny amount of ferromagnetic components. The magnetic properties of NiO nanostructures have been concluded to be highly dependent on the morphology.

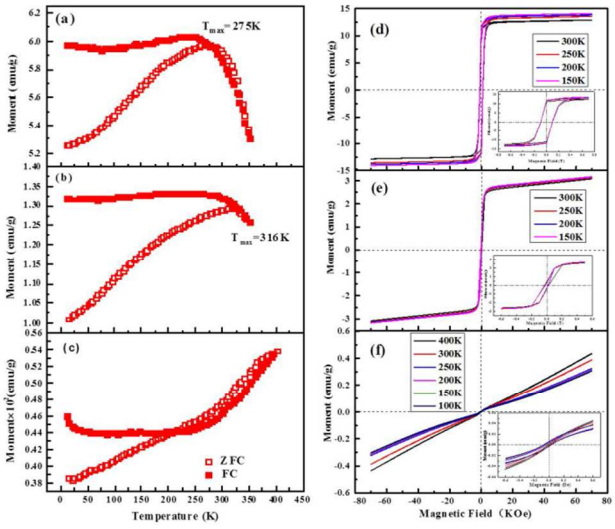

Fig. 7 Temperature dependence of the magnetization and Isothermal magnetization at several selected temperatures for NiO prepared at different pH values: (a) and (d) pH=9.30; (b) and (e) pH=10.30; (c) and (f) pH=10.90.

Conclusions

Nickel oxide (NiO) nanostructures with different morphologies have been successfully prepared via the hydrothermal synthesis, and their specific surface area and magnetic properties were investigated. It is found that different morphologies of the NiO, including nanoparticles, porous aggregates, and multi-shelled spheres, can be prepared by controlling the surface energy and growth rate through varying the pH values of the precursors with $NH_3{\cdot}H_2O$. The

investigation in the properties of as synthesized NiO products with different morphologies indicates that the morphology plays a crucial role in determining their surface area and the magnetic properties. Our findings provide an effective solution for tuning the morphology of NiO nanostructure, which will benefit for its applications.

Acknowledgements

This work was supported partially by the National Natural Science Foundation of China (91333122, 51372082, 51172069, 61204064 and 51202067), a grant from the Ph.D. Programs Foundation of Ministry of Education of China (20130036110012, 20110036110006), the Fundamental Research Funds for the Central Universities, and the Science and Technology Program Foundation of Suzhou City (SYG201215)

Notes and references

[a] State Key Laboratory of Alternate Electrical Power System with Renewable Energy Sources, School of Renewable Energy, North China Electric Power University, Beijing 102206, China. Email: mcli@ncepu.edu.cn

[b] Suzhou Institute, North China Electric Power University, Suzhou 215123, China.

[c] Institut Néel, CNRS and Université Joseph Fourier, BP 166, 38042 Grenoble, France.

1. X. L. Wang, P. S. Ku, Q. Shao, W. F. Cheng, C. W. Leung and A. Ruotolo, *Appl. Phys. Lett.*, 2013, **103**, 223508.
2. G. X. Zhu, H. Xu, Y. J. Liu, C. Y. Xi, J. Yang, X. Shen, J. Zhu and J. Yang, *J. Colloid Interf. Sci.*, 2013, **412**, 100.
3. L. Y. Lin, T. M. Liu, B. Miao and W. Zeng, *Mater. Res. Bull.*, 2013, **48**, 449.
4. Q. Dong, S. Yin, C. S. Guo, X. Y. Wu, N. Kumada, T. Takei, A. Miura, Y. Yonesaki and T. Sato, *Appl.Catal. B Environ.*, 2014, **147**, 741.
5. M. Y. Cheng, Y. S. Ye, T. M. Chiu, C. J. Pan and B. J. Hwang, *J. Power Sources*, 2014, **253**, 27.
6. Y. Q. Zhang, X. H. Xia, J. P. Tu, Y. J. Mai, S. J. Shi, X. L. Wang and C. D. Gu, *J. Power Sources*, 2012, **199**, 413.
7. J. Wang, H. Pang, J. Yin, L. Guan, Q. Lu and F. Gao, *CrystEngComm*, 2010, **12**, 1404.
8. H. Liu, X. N. Dong, C. Y. Duan, X. Su and Z. F. Zhu, Micro Nano Lett., 2013, **8**, 745.
9. Y. F. Cui, C. Wang, S. J. Wu, G. Liu, F. F. Zhang and T. M. Wang, *CrystEngComm*, 2011, **13**, 4930.
10. M. Y. Ge, L. Y. Han, U. Wiedwald, X. B. Xu, C. Wang, K. Kuepper, P. Ziemann and J. Z. Jiang, *Nanotechnology*, 2010, **21**, 425702.
11. D. Wang, P. Yang, Q. Ma, Y. Cao, A. Zhang and B. Huang, *CrystEngComm*, 2013, **15**, 8959.
12. M. Liu, J. Chang, J. Sun and L. Gao, *Electrochim. Acta*, 2013, **107**, 9.
13. X. Wang, L. Wan, T. Yu, Y. Zhou, J. Guan, Z. Yu, Z. Li and Z. Zou, *Mater. Chem. Phys.*, 2011, **126**, 494.
14. B. Cheng, Y. Le, W. Q. Cai and J. G. Yu, *J. Hazard. Mater.*, 2011, **185**, 889.
15. C. Pan, R. Ding, Y. Hu and G. Yang, *Physica E*, 2013, **54**, 138.
16. W. Shi, S. Song and H. Zhang, *Chem. Soc. Rev.*, 2013, **42**, 5714.
17. L. Wang, Y. J. Hao, Y. Zhao, Q. Y. Lai and X. Y. Xu, *J. Solid State Chem.*, 2010, **183**, 2576.
18. D. Sun, J. l. Zhang, H. J. Ren, Z. F. Cui and D. X. Sun, *J. Phys. Chem. C*, 2010, **114**, 12110.
19. Z. H. Liang, Y. J. Zhu and X. L. Hu, *J. Phys. Chem. B*, 2004, **108**, 3488.
20. C. Yuan, X. Zhang, L. Su, B. Gao and L. Shen, *J. Mater. Chem.*, 2009, **19**, 5772.
21. M.M. Titirici, M. Antonietti and A. Thomas, *Chem. Mater.*, 2006, **18**, 3808.
22. L. X. Yang , Y. J. Zhu, H. Tong , Z. H. Liang and W. W. Wang, *Cryst. Growth Des.*, 2007, **7** 2716.
23. X. W. Lou, C. Yuan and L. A. Archer, *Small*, 2007, **3**, 261.
24. W. Q. Cai, J. G. Yu, S. H. Gu and M. Jaroniec, *Cryst. Growth Des.,* 2010, **10**, 3977.
25. C. J. Jia, L. D. Sun, Z. G. Yan, L. P. You, F. Luo, X. D. Han, Y. C. Pang, Z. Zhang and C. H. Yan, *Angew. Chem., Int. Ed.* 2005, **44**, 4328.
26. X. Lai, J. E. Halpert and D. Wang, *Energ. Environ. Sci.*, 2012, **5**, 5604.
27. Z. Dong, X. Lai, J. E. Halpert, N. Yang, L. Yi, J. Zhai, D. Wang, Z. Tang and L. Jiang, *Adv. Mater.*, 2012, **24**, 1046.
28. M. P. Proenca, C. T. Sousa, A. M. Pereira, P. B. Tavares, J. Ventura, M. Vazquez and J. P. Araujo, *Phys. Chem. Chem. Phys.*, 2011, **13**, 9561.
29. H. Pang, Q. Y. Lu, Y. C. Lia and F. Gao, *Chem. Commun.*, 2009, **48**, 7542.
30. S. Farhadi and Z. R. Zaniyani, *Polyhedron*, 2011, **30**, 971.

Colour graphic:

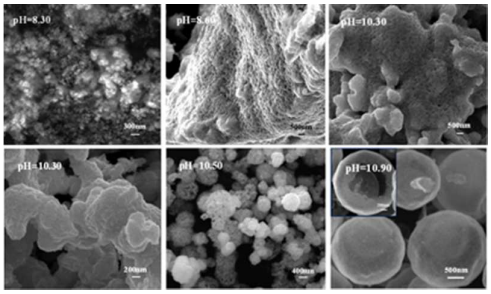

Text:

The morphology of NiO nanostructures was controlled by tuning pH value via hydrothermal process